European Journal of Medicinal Chemistry 90 (2015) 766–774

Contents lists available at ScienceDirect

European Journal of Medicinal Chemistry

journal homepage: http://www.elsevier.com/locate/ejmech

Original article

In vitro anticancer activity of gold(III) complexes with some esters of (*S*,*S*)-ethylenediamine-*N*,*N*′-di-2-propanoic acid

Nebojša Pantelić [a], Tatjana P. Stanojković [b], Bojana B. Zmejkovski [c], Tibor J. Sabo [d, **], Goran N. Kaluđerović [e, *]

[a] Faculty of Agriculture, University of Belgrade, Nemanjina 6, 11080 Belgrade-Zemun, Serbia
[b] Institute of Oncology and Radiology, 11000 Belgrade, Serbia
[c] Department of Chemistry, Institute of Chemistry, Technology and Metallurgy, University of Belgrade, Studenski Trg 14, 11000 Belgrade, Serbia
[d] Faculty of Chemistry, University of Belgrade, P. O. Box 158, 11001 Belgrade, Serbia
[e] Department of Bioorganic Chemistry, Leibniz-Institute of Plant Biochemistry, Weinberg 3, D 06120 Halle (Saale), Germany

ARTICLE INFO

Article history:
Received 11 July 2014
Received in revised form
9 December 2014
Accepted 11 December 2014
Available online 12 December 2014

Keywords:
Gold(III) complexes
R_2edda-type ligands
DFT
Apoptosis
Cell cycle
Cytotoxicity

ABSTRACT

Five novel gold(III) complexes of general formulas [$AuCl_2${(*S*,*S*)-R_2eddip}]PF_6, ((*S*,*S*)-eddip = (*S*,*S*)-ethylenediamine-*N*,*N*′-di-2-propanoate, *R* = *n*-Bu, *n*-Pe, *i*-Bu, *i*-Am, *c*Pe; **1**–**5**, respectively) were synthesized and characterized by UV/Vis, IR and NMR spectroscopy and mass spectrometry. DFT calculations indicated that (*R*,*R*)-*N*,*N*′-configuration diastereoisomers were the most stable for **1**–**5**. **3** is stable in DMSO for at least 24 h, but immediate hydrolysis in PBS occurs. **3** is readily reduced with ascorbic acid and forms adducts with bovine serum albumin (BSA). *In vitro* anticancer activity of the gold(III) complexes against human cervix adenocarcinoma HeLa, human myelogenous leukemia K562, human melanoma Fem-x tumor cell lines, as well as against non-cancerous human embryonic lung fibroblast cell line MRC-5 was determined using MTT assay. Complex **4** showed highest activity and selectivity (IC_{50}(Fem-x) = 1.3 ± 0.2; IC_{50}(MRC-5)/IC_{50}(Fem-x) = 72.5 ± 12.4), 4 times more active and 28 times more selective than cisplatin. Complexes induced apoptotic mode of death in a time-dependent manner in HeLa cells.

1. Introduction

The progress of medicinal inorganic chemistry includes several applications of a variety of metal complexes in medicine [1–4]. To design a metal-based applicable anticancer drug is challenging. Any candidate for an antitumor agent needs to demonstrate its positive reactions with target biomolecules and favorable physiological responses to tumors before entering clinical trials. Cisplatin has made an impressive impact on cancer chemotherapy, and nowadays is frequently used in treatment of various types of cancers [5–9]. Its activity, as well as activity of new-generation platinum compounds, is compromised due to inevitable serious side effects such as nephrotoxicity and neurotoxicity, hair and hear loss and many others [10–13]. Interest in medicinal chemistry of gold has been growing with the successful use of auranofin for treatment of rheumatoid arthritis [14,15]. Gold(III) complexes have greatly attracted researchers' attention in the last decade for their outstanding cytotoxic actions against different tumor cells [16,17], even against the cisplatin-resistant cell lines [18–20]. With square-planar geometry (d^8 system), gold(III) complexes are isoelectronic and isostructural to platinum(II) complexes, thus they could show a model of binding to the biomolecules similarly to cisplatin [21,22]. The strict relationship to platinum(II) compounds makes gold(III) complexes good candidates for development as anticancer drugs, although gold(III) complexes are not very stable under physiological conditions because of their high reduction potential and fast hydrolysis rate. These problems can possibly be circumvented by forming gold(III) compounds with one or more multidentate nitrogen-donor ligands to enhance their stability [23–25]. Recent findings by Messori et al. showed that most of the cytotoxic gold(III) complexes have a weak binding affinity to DNA, which is the primary target for platinum(II) antitumor drugs [22]. Also, it was found that cytotoxic gold(III) complexes have shown high reactivity toward different protein models [26]. Most of the known active gold(III) complexes might react through gold(I) species produced

* Corresponding author.
** Corresponding author.
E-mail addresses: tsabo@chem.bg.ac.rs (T.J. Sabo), goran.kaluderovic@ipb-halle.de (G.N. Kaluđerović).

http://dx.doi.org/10.1016/j.ejmech.2014.12.019
0223-5234/

by gold(III) reduction *in vivo* [27]. However, there are exceptions where e.g. porphyrinato ligand markedly stabilizes the gold(III) ion against reduction diminishing the possibility to be reduced by biological reductants such as glutathione and ascorbic acid [28].

Generally, very few gold(III) compounds demonstrate anticancer activity *in vivo* [29]. Since the early investigations on [AuX_2(damp)] (damp = 2-[(dimethylamino)methyl]-phenyl, X_2/X = malonato/acetato) [30,31], *in vivo* anticancer activity has been reported for only four other types of gold(III) compounds, gold(III) dithiocarbamate [32], gold(III) porphyrins [33,34], cyclometallated gold(III) NHC [35] and gold(III) phosphine complex [36].

Recently, synthesis and characterization of gold(III) complexes with esters of cyclohexyl-functionalized ethylenediamine-*N*,*N*′-diacetate was reported (Fig. 1) [37]. The *in vitro* cytotoxic evaluation of the investigated complexes against tumor cell lines: human adenocarcinoma (HeLa cells), human myelogenuos leukemia (K562 cells) and against normal peripheral blood mononuclear cells (PBMC), showed that the cytotoxic action of gold(III) complexes with cyclohexyl-functionalized ethylenediamine-*N*,*N*′-diacetate esters, (R = *i*-Bu, *i*-Am), is fairly comparable to that of cisplatin [37].

Inspired by these promising results, five novel gold(III) complexes of *N*,*N*′ bidentate (*S*,*S*)-R_2eddip ligands with general formulae [$AuCl_2${(*S*,*S*)-R_2eddip}]PF_6: ((*S*,*S*)-eddip = (*S*,*S*)-ethelendiamine-*N*,*N*′-di-2-propanoate; R = *n*-Bu, *n*-Pe, *i*-Bu, *i*-Am, *c*Pe, **1**–**5**, respectively) were synthesized. Density functional theory (DFT) analyses were performed for indication of the preferred configuration of nitrogen atoms. Stability of **3** in DMSO and in physiological medium (PBS) was examined, as well as possibility of reduction by ascorbic acid, by time-dependent UV/Vis spectrometry and ^{13}C NMR spectroscopy. Interaction of a selected complex, **3** with bovine serum albumin (BSA) is monitored by UV/Vis spectrometry over time. All compounds were tested against cervix adenocarcnoma cell line (HeLa), human chronic myelogenous leukemia (K562), human melanoma (Fem-x) and non-cancerous cell line, human embryonic lung fibroblast (MRC-5) with the aim of assessing *in vitro* activity and selectivity. The mode of HeLa cell death induced by **1**–**5** was also studied, as well as cell cycle distribution of HeLa cells upon treatment with these complexes.

2. Results and discussion

2.1. Chemistry

In the reaction of $Na[AuCl_4]\cdot 2H_2O$ and an equimolar amount of corresponding (*S*,*S*)-R_2eddip ligand, previously deprotonated with LiOH in methanol, and after addition of ammonium hexafluorophosphate to the reaction mixture, desired complexes **1**–**5** (Scheme 1) were obtained as yellow powders. The complexes are soluble in methanol, ethanol, acetone, dichloromethane, chloroform, dimethyl sulfoxide and acetonitrile.

2.2. Spectroscopic characterizations

IR spectra showed strong ν(C=O) absorption stretching bands from 1732 to 1738 cm^{-1} (**1**–**5**) [38,39], similarly to the corresponding free ligands [38–42], thus indicating that coordination of the carboxylic oxygen can be excluded. Asymmetric ν(–CH_3/–CH_2) vibrations of moderate intensities are found in the range 2867–2968 cm^{-1}. The ν(C–N) vibrations found at 845–849 cm^{-1} suggest that coordination occurred *via* nitrogen atoms [39]. The ν(Au–N) bands were found at 558–560 cm^{-1} for all complexes. Far-IR spectra of **1**–**3** show ν(Au–Cl) signals at 355, 357 and 360 cm^{-1}, respectively. Assignment of the Au–Cl and Au–N vibrational bands, confirmed with DFT calculations, are in agreement with literature data [39,43].

UV/Vis data showed absorption around 320 nm which corresponds to LMCT transitions and could be assigned to Cl → Au charge transfer by analogy to auric acid absorption spectra [44]. Similar electronic transitions are observed in analogous gold(III) complexes [37]. According to crystal field theory of d^8 complexes the LUMO orbital is $d(x^2\text{-}y^2)$, thus ligand to metal charge transfer could be due to $p_\sigma \rightarrow d(x^2-y^2)$ transition. Also, electronic spectra proved that these complexes are stable and that gold remains in oxidation state +3 [43]. ESI-MS were recorded in positive ion mode, and in all cases, the $[M-PF_6]^+$ peak was detectable.

NMR spectroscopic data supports suggested structures of **1**–**5** and *NN* bidentate coordination of (*S*,*S*)-R_2eddip esters [38,40–42,45–47]. Selected NMR data is listed in Table 1. In ^{1}H NMR spectra the broad signals of hydrogen atoms belonging to secondary amino groups appear between 7.30 and 8.10 ppm (comparing to ligand precursors *ca*. 10 ppm) [42]. The chemical shifts of CH_2 protons of the ethylenediamine bridge show coordination induced shifts (up to 0.5 ppm) giving a clear indication of nitrogen coordination. Resonances of cyclopentyl hydrogen atoms of **5** were found between 1.50 and 2.00 ppm, while protons from alkyl moieties from ester groups of **1**–**4** were located at below 2.10 ppm. Methyl hydrogen atoms from α-alaninato moiety were found at around 1.70 ppm. The CH_2O/(*c*Pe)CHO can be seen above 3.97 ppm, as expected [38,40,41,42]. In ^{13}C NMR spectra resonances of carbonyl carbon atoms around 170 ppm imply that oxygen atoms are not participating in coordination and also intact ester function. Complete characterization of complex **3**, as an example, can be seen in supplementary section (Figures S2–S6).

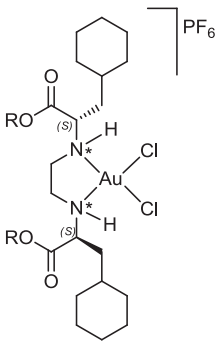

R = Me, Et, *n*-Pr, *n*-Bu, *i*-Bu, *i*-Am

Fig. 1. Complexes of gold(III) with cyclohexyl-functionalized R_2edda-type ligands.

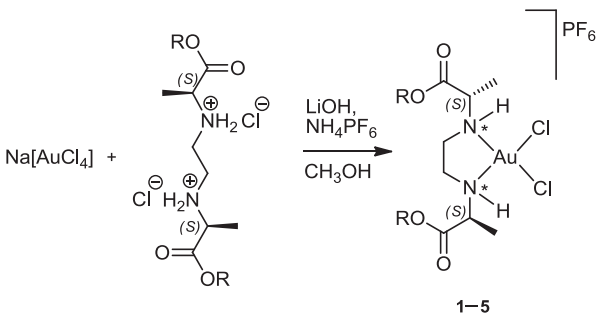

R = *n*-Bu, *n*-Pe, *i*-Bu, *i*-Am, *c*Pe

Scheme 1. Synthesis of gold(III) complexes **1**–**5**.

Table 1
Selected ^{1}H and ^{13}C NMR data (δ in ppm) for complexes, **1**–**5**.

Complexes	^{1}H			^{13}C			
	C***H***$_2$-(en)	C***H***	C***H***$_2$O/C***H***O	***C***H$_2$-(en)	***C***H	***C***OO	***C***H$_2$O/***C***HO
1	3.60–4.00	3.93	4.26	42.9	56.3	169.4	67.4
2	3.60–4.00	3.89	4.26	42.8	56.1	169.6	67.7
3	3.70–4.10	4.36	4.62	42.9	56.1	169.4	73.2
4	3.60–4.00	4.11	4.29	42.9	56.1	169.5	71.9
5	3.30–3.90	4.17	5.34	43.5	57.1	169.3	81.3

2.3. Quantum chemical calculations

DFT calculations were conducted for the isomers arising from κ^2*N*,*N*′ coordination of (*S*,*S*)-R$_2$eddip (*R* = *n*-Bu, *n*-Pe, *i*-Bu, *i*-Am, *c*Pe) to AuCl$_2$ fragment (denoted as **1c**–**5c**). Equilibrium structures are shown for **5c** as an example in Fig. 2 (for **1c**–**4c** see Figure S1). All structures were fully optimized without any symmetry constraints. The calculated results for all complexes, **1c**–**5c** showed that the (*R*,*R*)-*N*,*N*′ diastereoisomer is most stable. Namely, the energy difference between the (*R*,*R*)-**1c-5c** and (*R*,*S*) ≡ (*S*,*R*)-**1c**–**5c** diastereoisomer is around 1 kcal/mol, which is within the error of DFT calculations. These results are in agreement with those obtained for platinum(IV) complexes with R$_2$edda-type esters, where the structures were confirmed by X-ray analysis [38,48]. Although the difference in energies between (*R*,*R*) and (*R*,*S*) isomers are small this might be indication for the most stable isomer. The third isomer, (*S*,*S*)-**1c**–**5c** is 3.2–4.1 kcal/mol higher in energy than (*R*,*R*)-**1c**–**5c**. The results obtained by NMR spectroscopy (within the sensitivity limits of this method) revealed the presence of a single isomer (one set of signals) and DFT calculations indicated that it could be assigned as (*R*,*R*)-*N*,*N*′.

2.4. Stability and reactivity

The stability and reactivity experiments have been monitored by UV/Vis or NMR spectroscopy [49,50,51]. Complex **3** was selected and its stability was investigated in DMSO and physiological medium (PBS). UV/Vis spectra of **3** in DMSO correspond to the spectra recorded in $CHCl_3$ and there is no time-dependent appearance (24 h) of new absorption maximum. Stability studies of **3** in PBS examined by ^{13}C NMR spectroscopy at different time intervals (Figure S12) have been carried out, because chemical shift arising from water gave a very large and broad resonance which covered the part of the ^{1}H NMR spectra with characteristic chemical shifts for this class of gold(III) complexes. As it can be seen in Figure S12, addition of PBS immediately (0 h) causes coordination changes in **3** which presumably indicates instant coordination of water by displacement of the chlorido ligands to give the species [AuCl(H$_2$O){(*S*,*S*)-(*i*-Bu)$_2$eddip}]$^{2+}$ or [Au(H$_2$O)$_2${(*S*,*S*)-(*i*-Bu)$_2$eddip}]$^{3+}$ [52].

Cellular reducing substances such as ascorbic acid and thiol-containing species like metallothioneins and glutathione might be regarded as activators of gold(III) prodrugs [28,53,54]. In order to investigate possibility that [AuCl$_2${(*S*,*S*)-(*i*-Bu)$_2$eddip}]$^{+}$ is reduced in cells with biological relevant reductant, time-depending ^{13}C NMR spectroscopy was performed for the reaction of **3** with ascorbic acid. As it could be seen in Figure S11, ascorbic acid reduces the complex readily and instantly, indicating a high possibility of the same outcome in living cells.

Metal ions bind to albumins and it is suggested that metal-BSA adduct formation occurs through coordination of surface histidines and/or cysteines [55,56]. Furthermore, gold compounds are found to react with *S*-donors such as methionine and the Cys34 residues of albumin [57]. The interaction of **3** with bovine serum albumin was examined by UV/Vis spectrometry. Spectra are shown (Fig. 3) for certain time points with different used concentrations of **3** (**a**–**e**). According to Espósito et al. [57], it is assumed that [AuCl$_2${(*S*,*S*)-(*i*-Bu)$_2$eddip}]$^{+}$ might be reduced with cysteine leading to gold(I) complex as inferred through the disappearance of the LMCT gold(III) absorption (ca. 320 nm) as seen after 2 h of reaction (Fig. 3). After 24 and 48 h, UV/Vis spectra indicate that gold(I) species might disproportionate to corresponding gold(III) complex and elemental gold [58]. Consistent with the literature, complex **3** seems to react in similar manner as [Au(en)Cl$_2$]$^{+}$. Moreover, appearance of absorption band (540 nm) indicates formation of elemental gold [59].

2.5. Cytotoxic activity

Complexes **1**–**5** were tested for their cytotoxic activity *in vitro* against three human cancer cell lines: HeLa cervix adenocarcinoma, Fem-x human melanoma, K562 human chronic myelogenous leukemia, as well as on non-cancerous MRC-5 human embryonic lung fibroblast cells. The results of *in vitro* cytotoxic activity are expressed as IC$_{50}$ (the concentration of compound (in μM) that inhibits a proliferation rate of the tumor cells by 50% as compared to control untreated cells) and presented in Table 2.

In Fig. 4 is depicted survival of HeLa, Fem-x, K562 and non-cancerous MRC-5 cells grown for 72 h in the presence of increasing concentrations of gold(III) compounds. Complexes **1**–**5** exhibit high activity against all three cancer cell lines, the highest against Fem-x cells. The lowest IC$_{50}$ value is observed against Fem-x cells by complex **4** and at the same time the highest, against HeLa and K562. Complex **2** is found to be the most active against all cancer cell lines (Table 2). The IC$_{50}$ values range from 1.3 to 5.0 μM, and are compared to the corresponding IC$_{50}$ for cisplatin (Table 2).

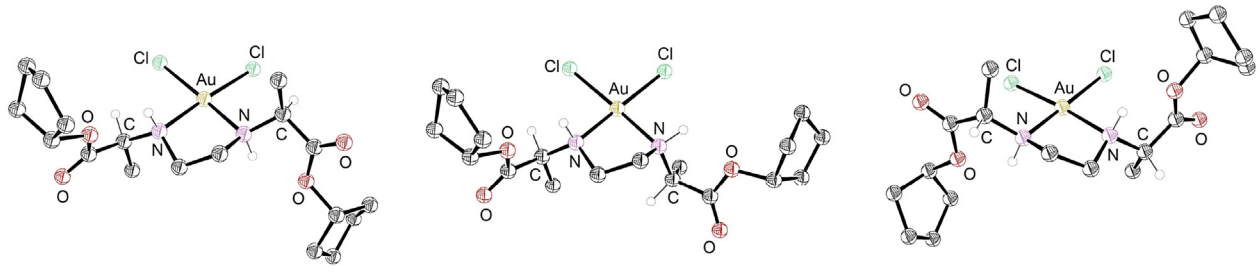

Fig. 2. Calculated structures of **5c**, as an example. H atoms, except those bonded to chiral atoms, are omitted for clarity.

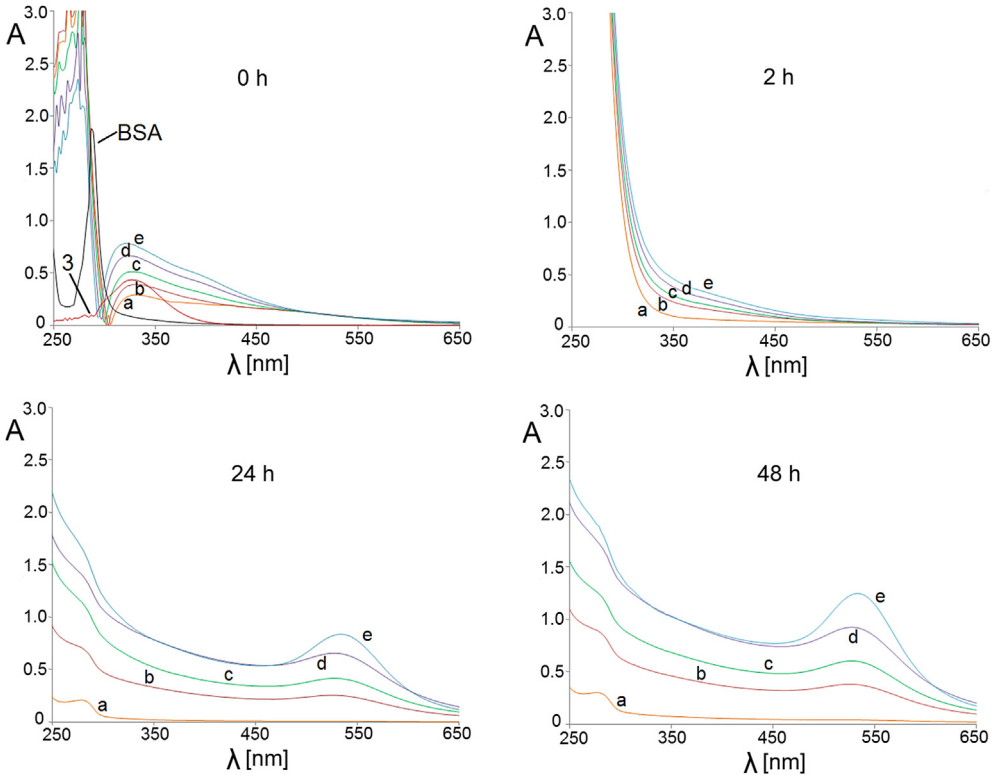

Fig. 3. Interaction of **3** with BSA followed by UV/Vis spectrometry over time. Concentrations of **3**: $1 \cdot 10^{-3}$; a–e: $1 \cdot 10^{-4} - 5 \cdot 10^{-4}$, respectively; BSA: $4 \cdot 10^{-6}$ mol/dm^3.

Table 2
IC_{50} [μM][a] concentrations of complexes **1**–**5** against HeLa, Fem-x, K562 and MRC-5 cells.

Complexes	IC $_{50}$ [μM]			
	HeLa	Fem-x	K562	MRC-5
1	2.07 ± 0.15	2.01 ± 0.31	2.97 ± 0.35	23.15 ± 0.85
2	1.61 ± 0.11	1.39 ± 0.08	1.45 ± 0.83	84.46 ± 0.24
3	1.99 ± 0.81	1.78 ± 0.35	4.41 ± 0.42	56.77 ± 1.26
4	2.14 ± 0.76	1.35 ± 0.23	5.01 ± 0.15	97.88 ± 1.75
5	1.72 ± 0.67	1.57 ± 0.24	2.69 ± 0.33	61.55 ± 2.35
Cisplatin	2.10 ± 0.20	5.51 ± 0.31	5.54 ± 1.03	14.21 ± 1.54

[a] Mean values ± SD (standard deviation) from three experiments.

It could be seen that novel gold(III) complexes are mostly more efficient than cisplatin against Fem-x and K562 tumor cell lines, while similar activity was observed against HeLa cells.

Introducing gold(III) as the metal center in this system of metal complexes with R_2edda-type ligands has a positive impact on the antiproliferative action, since platinum(II) and platinum(IV) complexes have shown lower activity in previous research [38,48].

Activities of **3** and **5** are considerably higher in comparison to free ligand-precursors ($IC_{50} = 82.8–180.9$ μM) [29,31], which is not the case for **1**, **2** and **4** where cytotoxicities are slightly lower or comparable depending on cell line ($IC_{50} = 1.51–5.22$ μM) [42]. On the other hand, $Na[AuCl_4]$ shows much lower antitumor activity [60].

2.6. Selectivity

Against the non-cancerous lung fibroblasts (MRC-5) all tested complexes were significantly less toxic than cisplatin and did not exert any essential cytotoxic action on normal cells with IC_{50} doses determined for investigated tumor cell lines. Selectivity indices are calculated and given in Table 3. Selectivities of these new complexes are much greater than cisplatin and similar platinum(IV/II) complexes [38].

These results reveal that complexes **1**–**5** exhibit a high degree cytotoxic activity against cancerous cells with great selectivity (Tables 2 and 3). With 4 times higher activity on Fem-x cells and 28 times higher selectivity than cisplatin, complex **4** is very promising candidate for further stages of screening *in vitro* and/or *in vivo*.

2.7. Cell cycle effects

The effect of complexes **1**–**5** on cell cycle progression was investigated in HeLa cells. Cell cycle was assessed by cytofluorimetric analysis, using propidium iodide (PI) to label DNA (Fig. 5). Flow cytometry with PI staining showed no significant increase in the number of cells in sub-G1 phase, and accordingly no significant difference in cell cycle distribution after 24 h of continuous action. Especially, incubation of the cell line HeLa with complexes **1**–**5** induced a very slight accumulation of cells in S phase. On the contrary, for 48 h treatment it is observed that complexes **1**–**5** induced the accumulation of significant number of cells in the sub-G1 and S-phase arrest (Fig. 5). These results indicated that the observed growth inhibitory effects of investigated compounds might be due to cell cycle arrest, and is accompanied by a decrease in G2/M phase cells in a time-dependent manner (Fig. 5). These results suggest that the investigated gold(III) complexes could act inhibiting cell entry in mitosis.

2.8. Morphological study

The results from fluorescence microscopy of complexes **1**–**5** treated HeLa cells coupled with AO/EB double staining for the occurrence of morphological changes and DNA condensation are

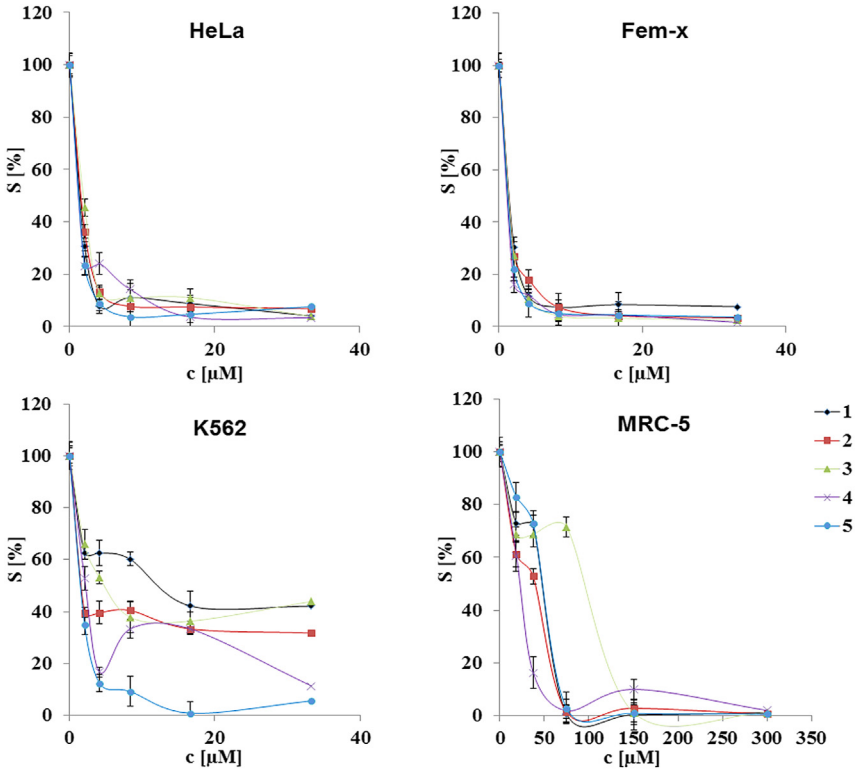

Fig. 4. Representative graphs show survival of HeLa, Fem-x, K562 and MRC-5 cells grown for 72 h in presence of increasing concentrations of investigated compounds, determined by MTT test.

presented in Fig. 6. HeLa cells were collected after treatment, in order to determine the cells that are categorized as viable, early apoptotic, late apoptotic or autophagic.

The data shows that compounds (IC_{50}) triggered morphological changes in treated HeLa cells that indicated possible induction of apoptosis upon treatment. The presence of intercalated AO within fragmented DNA indicates early apoptosis. At 24 h after treatment with complexes **1**–**5** blebbing and nuclear chromatin condensation were noticeable. Late apoptosis is indicated by the presence of reddish orange (in web version) color due to the binding of AO to denatured DNA as observed (Fig. 6). Because cells treated with complexes **1**, **2** or **4** showed signs that might be associated with autophagy (Fig. 6), additional tests were done in order to determine if the autophagic process is activated after treatment of HeLa cells with mentioned complexes. Flow cytometric analysis indicated that autophagy was not triggered upon the treatment with investigated complexes (Figure S13).

3. Conclusions

Synthesis of five novel gold(III) complexes, $[AuCl_2\{(S,S)\text{-}R_2eddip\}]PF_6$, R = *n*-Bu, *n*-Pe, *i*-Bu, *i*-Am, *c*Pe, **1**–**5**, respectively, was described. The compounds were characterized by elemental analysis, UV/Vis, IR, NMR spectroscopy and mass spectrometry. Spectroscopic data suggest ligand chelation *via* nitrogen donor atoms. NMR spectra show presence of one isomer. DFT calculations indicate that (*R*,*R*)-*N*,*N*′- diastereoisomer is the most stable one. Complex **3** was stable in DMSO but in physiological medium (PBS) immediately causes displacement of the chlorido ligands by water molecules. **3** reacts with ascorbic acid readily and instantly, indicating a high possibility of the same outcome in living cells. Metal–protein adducts are formed by interaction of **3** with BSA. All investigated compounds were tested for *in vitro* antiproliferative activity against human adenocarcinoma HeLa, human myelogenous leukemia K562, human melanoma Fem-x tumor cell lines and non-cancerous human embryonic lung fibroblast cell line MRC-5. Complexes exhibited high cytotoxic activity against all three cancer cell lines, against Fem-x and K562 even higher than cisplatin. All complexes were significantly less toxic (against normal MRC-5 cells) than cisplatin. Complex **4** showed highest activity and selectivity (IC_{50}(Fem-x) = 1.3 μM; IC_{50}(MRC-5)/IC_{50}(Fem-x) = 72.5), 4 times more active and 28 times more selective than cisplatin. The observed growth inhibitory effects of investigated compounds on HeLa cells might be due to cell cycle arrest, and is accompanied by a decrease in G2/M phase cells in a time-dependent manner. Consequently, apoptosis is main mode of cell death in HeLa cells induced by **1**–**5** gold(III) complexes.

4. Experimental

4.1. Materials and methods

The *n*-butyl, *n*-pentyl, isobutyl, isoamyl and cyclopentyl esters of (*S*,*S*)-ethylenediamine-*N*,*N*′-di-3-propanoic acid were synthesized according to described method [38,40–42]. $Na[AuCl_4]$ was synthesized by the standard procedure [61].

Elemental analyses were performed on an Elemental Vario EL III microanalyzer. A Nicolet 6700 FT–IR spectrometer and ATR technique were used for recording mid-infrared spectra (4000–400 cm^{-1}) for all complexes. Far-IR spectra were recorded at room temperature in the range of 600–150 cm^{-1}, using ATR technique on the same instrument with Far-IR beam splitter. NMR spectra were recorded on Varian Gemini 200 or Bruker Avance III 500 spectrometers. Chemical shifts for ^1H and ^{13}C NMR spectra were referenced to residual ^1H and ^{13}C present in $CDCl_3$. Mass spectra of complexes **1**–**4** were recorded with a 6210 Time-of-

Table 3
Selectivity index.

Complex	IC_{50}(MRC-5)/IC_{50}(cell line)		
	HeLa	Fem-x	K562
1	11.18 ± 0.91	11.52 ± 1.83	7.79 ± 0.96
2	52.46 ± 3.59	60.76 ± 3.50	58.25 ± 33.34
3	28.53 ± 11.63	31.89 ± 6.31	12.87 ± 1.26
4	45.74 ± 16.26	72.50 ± 12.42	19.54 ± 0.68
5	35.78 ± 14.01	39.20 ± 6.18	22.88 ± 2.94
Cisplatin	6.77 ± 0.98	2.58 ± 0.31	2.56 ± 0.55

After 1 h of stirring, deprotonated ligand dissolved completely. Then, 4 ml of $Na[AuCl_4]\cdot 2H_2O$ (0.050 g, 0.126 mmol) solution in methanol was introduced in the flask, followed by addition of solid NH_4PF_6 (0.062 g, 0.378 mmol). The solution is then evaporated under *vacuum* and the yellow product is washed with excess of water. Reaction was performed in the dark at room temperature.

Complex **1**. Yield 50 mg, 55%. Anal. calcd. for $C_{16}H_{32}N_2O_4AuCl_2PF_6$: C, 26.35; H, 4.42; N, 3.84%. Found: C, 26.24; H, 4.64; N, 3.76%. ^{1}H NMR (200 MHz, $CDCl_3$): 0.95 (t, 6H, $CH_3CH_2CH_2CH_2$—OOC—), 1.39 (q, 4H, $CH_3CH_2CH_2CH_2$—OOC—), 1.71

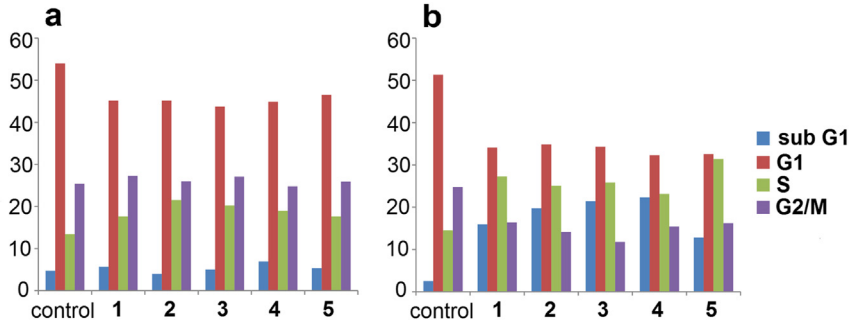

Fig. 5. Effect of compounds on cell cycle phase distribution: HeLa cell lines were exposed to IC_{50} doses of gold(III) compounds for 24 h (a) and 48 h (b).

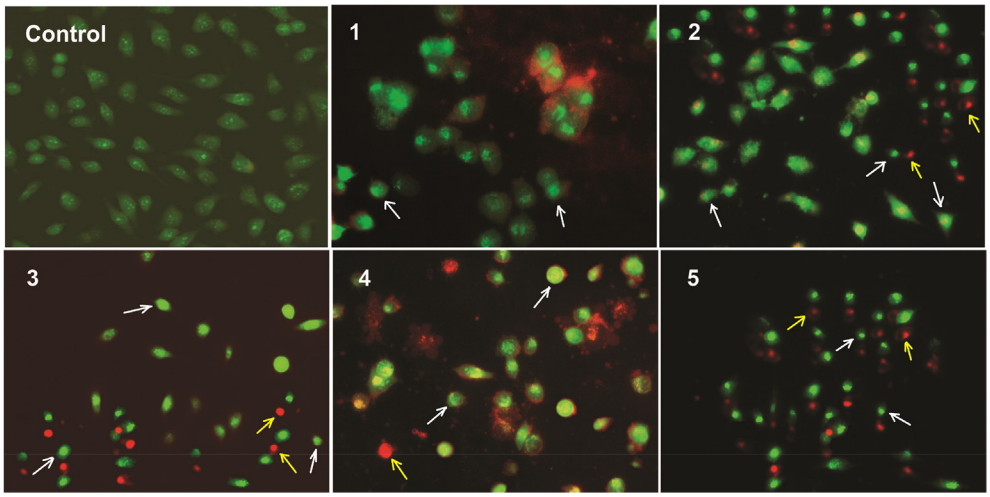

Fig. 6. Photomicrographs of acridine orange/ethidium bromide-stained HeLa cells untreated and treated with IC_{50} concentrations of investigated **1**–**5** compounds for 24 h (arrows: white – early apoptosis, yellow – late apoptosis). (For interpretation of the references to colour in this figure legend, the reader is referred to the web version of this article.)

Flight LC—MS instrument (G1969A, Agilent Technologies) in CH_3CN, and for complex **5** with an Orbitrap LTQ XL instrument (Thermo Scientific, Bremen, Germany) in CH_3OH. GBC UV/Vis Cintra 6 spectrometer was used for electronic spectra of complexes dissolved in $CHCl_3$ at 1×10^{-4} M, GBC UV/Vis Cintra 40 spectrometer was used for following interaction of **3** with BSA and evaluation of its stability in DMSO. Reagents and solvents were of commercial reagent grade quality and used without further purification.

4.2. Synthesis of complexes $[AuCl_2\{(S,S)\text{-}R_2eddip\}]PF_6$, ***1*–*5***

0.126 mmol of each ligand, $[(S,S)\text{—}H_2R_2eddip\}]Cl_2$, R = *n*-Bu (0.049 g), or *n*-Pe (0.053 g), or *i*-Bu (0.049 g), or *i*-Am (0.053 g) and or *c*Pe (0.052 g), **L1**·2HCl – **L5**·2HCl, respectively, was suspended in methanol (4 ml) and $LiOH\cdot H_2O$ (0.011 g, 0.252 mmol) was added. After 1 h of stirring, deprotonated ligand dissolved completely. Then, 4 ml of $Na[AuCl_4]\cdot 2H_2O$ (0.050 g, 0.126 mmol) solution in methanol was introduced in the flask, followed by addition of solid NH_4PF_6 (0.062 g, 0.378 mmol). The solution is then evaporated under *vacuum* and the yellow product is washed with excess of water. Reaction was performed in the dark at room temperature.

Complex **1**. Yield 50 mg, 55%. Anal. calcd. for $C_{16}H_{32}N_2O_4AuCl_2PF_6$: C, 26.35; H, 4.42; N, 3.84%. Found: C, 26.24; H, 4.64; N, 3.76%. ^{1}H NMR (200 MHz, $CDCl_3$): 0.95 (t, 6H, $CH_3CH_2CH_2CH_2$—OOC—), 1.39 (q, 4H, $CH_3CH_2CH_2CH_2$—OOC—), 1.71 (m, 10H, CH_3, $CH_3CH_2CH_2CH_2$—OOC—), 3.60–4.00 (m, 4H, CH_2-(en)), 4.26 (m, 6H, *CH*, $CH_3CH_2CH_2CH_2$—OOC—), 7.75 (s, 2H, N*H*). ^{13}C NMR (50 MHz, $CDCl_3$): 13.6 (CH_3), 14.8 ($CH_3CH_2CH_2CH_2$—OOC—), 18.9 ($CH_3CH_2CH_2CH_2$—OOC—), 30.2 ($CH_3CH_2CH_2CH_2$—OOC—), 42.9 (CH_2-(en)), 56.3 (*CH*), 67.4 ($CH_3CH_2CH_2CH_2$—OOC—), 169.4 ($CH_3CH_2CH_2CH_2$—OOC—). IR (ATR, cm^{-1}): 2963, 2874, 1738, 1455, 1236, 847. Far IR (ATR, cm^{-1}): 559, 355. UV/Vis ($CHCl_3$): λ_{max} = 318 nm. ESI—MS (CH_3CN), positive: m/z: 583.1405 $[M-PF_6]^+$.

Complex **2**. Yield 50 mg, 52%. Anal. calcd. for $C_{18}H_{36}N_2O_4AuCl_2PF_6\cdot H_2O$: C, 27.88; H, 4.94; N, 3.61%. Found: C, 27.43; H, 4.90; N, 3.89%. ^{1}H NMR (200 MHz, $CDCl_3$): 0.91 (t, 6H, $CH_3CH_2CH_2CH_2CH_2$—OOC—), 1.35 (m, 8H, $CH_3CH_2CH_2CH_2CH_2$—OOC—), 1.70 (m, 10H, CH_3, $CH_3CH_2CH_2CH_2CH_2$—OOC—), 3.60–4.00 (m, 4H, CH_2-(en)), 4.25 (m, 6H, *CH*, $CH_3CH_2CH_2CH_2CH_2$—OOC—) 7.88 (s, 2H, N*H*). ^{13}C NMR (50 MHz,

$CDCl_3$): 13.9 (CH_3), 14.8 ($CH_3CH_2CH_2CH_2CH_2$–OOC–), 22.2 ($CH_3CH_2CH_2CH_2CH_2$–OOC–), 27.8 ($CH_3CH_2CH_2CH_2CH_2$–OOC–), 27.9 ($CH_3CH_2CH_2CH_2CH_2$–OOC–), 42.8 (CH_2-(en)), 56.1 (CH), 67.7 ($CH_3CH_2CH_2CH_2CH_2$–OOC–), 169.6 ($CH_3CH_2CH_2CH_2CH_2$–OOC–). IR (ATR, cm^{-1}): 2960, 2867, 1737, 1455, 1232, 849. Far IR (ATR, cm^{-1}): 559, 357. UV/Vis ($CHCl_3$): λ_{max} = 318 nm. ESI–MS (CH_3CN), positive: *m/z*: 611.1718 $[M-PF_6]^+$.

Complex **3**. Yield 55 mg, 60%. Anal. calcd. for $C_{16}H_{32}N_2O_4AuCl_2PF_6$: C, 26.35; H, 4.42; N, 3.84%. Found: C, 26.80; H, 4.60; N, 4.13%. ^{1}H NMR (200 MHz, $CDCl_3$): 0.97 (d, 12H, $(CH_3)_2CHCH_2$–OOC–), 1.76 ('d', 6H, CH_3), 2.03 (m, 2H, $(CH_3)_2CHCH_2$–OOC–), 3.70–4.10 (m, 4H, CH_2-(en)), 4.36 (m, 2H, CH), 4.62 (br s, 4H, $(CH_3)_2CHCH_2$–OOC–) 8.10 (br s, 2H, NH). ^{13}C NMR (50 MHz, $CDCl_3$): 15.0 (CH_3), 19.0 ($(CH_3)_2CHCH_2$–OOC–), 27.5 ($(CH_3)_2CHCH_2$–OOC–), 42.9 (CH_2-(en)), 56.3 (CH), 73.2 ($(CH_3)_2CHCH_2$–OOC–), 169.4 ($(CH_3)_2CHCH_2$–OOC–). IR (ATR, cm^{-1}): 2968, 2879, 1735, 1464, 1231, 847. Far IR (ATR, cm^{-1}): 558, 360. UV/Vis ($CHCl_3$): λ_{max} = 326 nm, (CH_3OH): λ_{max} = 327 nm, (DMSO): λ_{max} = 321 nm. ESI–MS (CH_3CN), positive: *m/z*: 583.1417 $[M-PF_6]^+$. Spectra are given in supplementary section, Figures S2–S6.

Complex **4**. Yield 55 mg, 57%. Anal. calcd. for $C_{18}H_{36}N_2O_4AuCl_2PF_6 \cdot H_2O$: C, 27.88; H, 4.94; N, 3.61%. Found: C, 27.44; H, 4.84; N, 3.43%. ^{1}H NMR (200 MHz, $CDCl_3$): 0.93 (d, 12H, $(CH_3)_2CHCH_2CH_2$–OOC–), 1.40–1.70 (m, 6H, $(CH_3)_2CHCH_2CH_2$–OOC–, $(CH_3)_2CHCH_2CH_2$–OOC–), 1.73 (d, 6H, CH_3) 3.60–4.00 (m, 4H, CH_2-(en)), 4.11 (m, 2H, CH), 4.29 (m, 4H, $(CH_3)_2CHCH_2CH_2$–OOC–), 7.79 (s, 2H, NH). ^{13}C NMR (50 MHz, $CDCl_3$): 14.9 (CH_3), 16.2 ($(CH_3)_2CHCH_2CH_2$–OOC–), 22.3 ($(CH_3)_2CHCH_2CH_2$–OOC–), 33.9 ($(CH_3)_2CHCH_2CH_2$–OOC–), 42.9 (CH_2-(en)), 56.1 (CH), 71.9 ($(CH_3)_2CHCH_2CH_2$–OOC–), 169.5 ($(CH_3)_2CHCH_2CH_2$–OOC–). IR (ATR, cm^{-1}): 2961, 2873, 1739, 1461, 1227, 849. UV/Vis ($CHCl_3$): λ_{max} = 322 nm. ESI–MS (CH_3CN), positive: *m/z*: 611.1714 $[M-PF_6]^+$.

Complex **5**. Yield 59 mg, 62%. Anal. calcd. for $C_{18}H_{32}N_2O_4AuCl_2PF_6 \cdot H_2O$: C, 28.03; H, 4.44; N, 3.63%. Found: C, 28.10; H, 4.31; N, 3.67%. ^{1}H NMR (200 MHz, $CDCl_3$): 1.50–2.00 (m, 22H, CH_2–*c*Pe, CH_3), 3.30–3.90 (m, 4H, CH_2-(en)), 4.19 (q, 2H, CH), 5.34 (m, 2H, CH–*c*Pe), 7.30–7.80 (br s, 2H, NH). ^{13}C NMR (50 MHz, $CDCl_3$): 14.8 (CH_3), 23.6 (CH_2–*c*Pe), 32.5 (CH_2–*c*Pe), 43.5 (CH_2-(en)), 57.1 (CH), 81.3 (CH–*c*Pe), 169.3 (COO–*c*Pe). IR (ATR, cm^{-1}): 2966, 2875, 1732, 1452, 1242, 845. UV/Vis ($CHCl_3$): λ_{max} = 332 nm. ESI–MS (CH_3OH), positive: *m/z*: 607.1405 $[M-PF_6]^+$.

4.3. Computational details

Geometry optimizations were performed with the Gaussian 09 package [62]. All structures were optimized using the B3LYP functional [63]. The Stuttgart/Dresden (SDD) basis set for all atoms was employed in the calculations [64,65]. All systems were optimized without symmetry restrictions. The resulting geometries were characterized as equilibrium structures by the analysis of the force constants of normal vibrations. Supplementary data associated with the quantum chemical calculations can be obtained from the authors upon request.

4.4. Stability of **3** in physiological conditions and DMSO

Complex **3** (20 mg, 0.027 mmol) was dissolved in 0.4 ml of acetone-d_6 and ^{13}C NMR spectrum recorded. Afterward, 0.04 ml of phosphate buffered saline (PBS) solution (pH 7.4) was added (acetone-**3**: PBS = 10: 1) and their ^{13}C NMR spectra were recorded at room temperature at different time intervals (immediately, 2, 24 and 48 h).

Stability was also followed in DMSO over time for **3** by UV/Vis spectrometry. Fresh solution of **3** ($c = 1 \cdot 10^{-3}$ mol/dm^3) in DMSO was recorded immediately, after 5 min, 15 min, 2 h and 24 h. Absorption maximum is observed at λ_{max} = 321 nm. There was no change in UV/Vis spectra after 24 h.

4.5. Reduction of **3** with ascorbic acid

In an NMR tube containg 20 mg of **3**, (0.027 mmol), dissolved in 0.4 ml deuterated acetone, 60 mg of ascorbic acid (0.336 mmol, excess, molar ratio 1:12) was added. ^{13}C NMR spectra were recorded before and after addition (immediately, 2, 24 and 48 h) of ascorbic acid.

4.6. Interaction of **3** with BSA

Stock solution of **3** ($c = 3.33 \cdot 10^{-3}$ mol/dm^3) was prepared in methanol. Investigated samples were obtained using same concentration of BSA ($4 \cdot 10^{-6}$ mol/dm^3) in PBS (pH 7.4) and different concentrations of the gold(III) complex **3** ($1 \cdot 10^{-4}$, $2 \cdot 10^{-4}$, $3 \cdot 10^{-4}$, $4 \cdot 10^{-4}$ and $5 \cdot 10^{-4}$ mol/dm^3). Explicitly, different aliquots of stock solution of **3** (0.3, 0.6, 0.9, 1.2, 1.5 ml) were added to 5 ml of a $8 \cdot 10^{-6}$ mol/dm^3 BSA solution in PBS and the volumetric flask was filled with PBS up to 10 ml. These solutions were prepared freshly and UV/Vis spectra were recorded immediately and after 2, 24 and 48 h.

4.7. Biological studies

4.7.1. Preparation of drug solutions

A solution of the studied gold(III) complexes was prepared in DMSO (Sigma Aldrich) at a concentration of 20 mM and diluted by nutrient medium to various working concentrations. Nutrient medium was RPMI-1640 (PAA Laboratories) supplemented with 10% fetal bovine serum (Biochrom AG) and penicillin/streptomycin (PAA Laboratories).

4.7.2. Cell lines

Cervix adenocarcinoma cell line (HeLa), human melanoma (Fem-x), human chronic myelogenous leukemia (K562) cells, and a non-cancerous cell line, MRC-5 (human embryonic lung fibroblast) were grown in RPMI-1640 medium (Sigma). Media were supplemented with 10% fetal bovine serum, L-glutamine, and penicillin-streptomycin (Sigma).

4.7.3. Treatment of cell lines

Target cells HeLa (2000 cells per well), Fem-x (5000 cells per well), K562 (5000 cells per well), and non-cancerous MRC-5 (5000 cells per well) were seeded into wells of a 96-well flat-bottomed microtitre plate. Twenty-four hours later, after the cell adherence, different concentrations of investigated compounds were added to the wells, except for the control cells to which a nutrient medium only was added. The final concentrations range chosen was 1–100 μM (1, 8.25, 16.5, 33, and 100 μM). The final concentration of DMSO solvent never exceeded 0.5%, which was non-toxic to the cells. Especially, compounds were applied to the suspension of K562 cells 2 h after the cell seeding. All concentrations were set up in triplicate. Nutrient medium with corresponding concentrations of investigated compounds, but without cells, was used as a blank, also in triplicate. The cultures were incubated for 72 h.

4.7.4. Determination of cell survival

The effect of the prepared compounds on cancer cell survival was determined by the microculture tetrazolium test (MTT) according to Mosmann [66] with modification by Ohno and Abe [67] 72 h after addition of the compounds, as described earlier. Briefly,

20 mL of MTT solution (5 mg/ml phosphate-buffered saline) was added to each well. Samples were incubated for a further 4 h at 37 °C in a humidified atmosphere of 95% air/5% CO_2 (v/v). Then 100 ml of 100 g/L sodium dodecyl sulfate was added to extract the insoluble product formazan resulting from conversion of the MTT dye by viable cells. The number of viable cells in each well was proportional to the intensity of the absorbance of light, which was read in an enzyme-linked immunosorbent assay (ELISA) plate reader at 570 nm. The absorbance (A) at 570 nm was measured 24 h later. To determine cell survival (%), the A of a sample with cells grown in the presence of various concentrations of the investigated compounds was divided by the control optical density (the A of control cells grown only in nutrient medium) and multiplied by 100. It was implied that the A of the blank was always subtracted from the A of the corresponding sample with target cells. IC_{50} was defined as the concentration of an agent inhibiting cell survival by 50% compared with a vehicle-treated control. As positive control cisplatin was used. All experiments were done in triplicate.

4.7.5. Cell cycle analysis

Cervix adenocarcinoma cell line (HeLa), human melanoma (Fem-x) and human chronic myelogenous leukemia (K562) cells, were seeded in six-well plates (3×10^5 cells/well), and after 24 h treated with investigated compounds, except control cells, and incubated at 37 °C for the next 24 h. Concentrations used corresponded to IC_{50} values. After the incubation, the cells were collected by trypsinization, and fixed in ice-cold 70% ethanol for 1 h on ice, then at −20 °C for at least a week. After fixation, the cells were washed in PBS and pellets obtained by centrifugation were treated with RNAse (100 μg/ml) at 37 °C temperature for 30 min and then incubated with propidium iodide (PI) (40 μg/ml) for at least 30 min. DNA content and cell-cycle distribution were analyzed using a Becton Dickinson FACSCalibur flow cytometer. Flow cytometry analysis was performed using a CellQuestR (Becton Dickinson, San Jose, CA, USA) software on a minimum of 10,000 cells per sample [68].

4.7.6. Morphological analysis (AO/EB double staining)

Investigated compounds induced cell death in malignant cells was determined using acridine orange (AO) and ethidium bromide (EB), double staining according to standard procedures and examined under a fluorescence microscope [69]. HeLa cells were seeded overnight on coverslips (100,000 cells) in 2 ml of complete medium. The next day, cells were treated with IC_{50} of the investigated compounds for 24 h. After this period, coverslips with target cells were stained with acridine orange/ethidium bromide mixture (3 μg/ml AO and 10 μg/ml EB in PBS), and visualized under a fluorescence microscope (Fluorescence microscope-PALM MicroBeam systems-Carl Zeiss).

4.7.7. Acridine orange staining

Autophagy is characterized by the formation of acidic vesicular organelles (AVOs). To detect AVOs, vital staining with acridine orange was performed. Briefly, 3×10^5 cells/well were seeded in six-well plates and allowed to attach. The cells were treated with compounds for 24 and 48 h. The cells were collected by trypsinization, and then incubated with 1 mg/l acridine orange at 37 °C for 15 min. After that, the cells were washed twice in PBS. The stained cells were then analyzed using Becton Dickinson FACSCalibur flow cytometer and CellQuestR (Becton Dickinson, San Jose, CA, USA) software on a minimum of 10,000 cells per sample.

Acknowledgments

This research was supported by the Ministry of Education, Science and Technological Development of the Republic of Serbia, grant numbers 172035 and 175011. The authors thank D. Vučetić, Department of Chemistry, Institute of Chemistry, Technology and Metallurgy, University of Belgrade, for his help in NMR spectroscopy.

Appendix A. Supplementary data

Supplementary data related to this article can be found at http://dx.doi.org/10.1016/j.ejmech.2014.12.019.

References

[1] B. Lippert, Prog. Inorg. Chem. 37 (1989) 1–97.
[2] E.R. Jamieson, S.J. Lippard, Chem. Rev. 99 (1999) 2467–2498.
[3] M.J. Clarke, F. Zhu, D.R. Frasca, Chem. Rev. 99 (1999) 2511–2533.
[4] M.J. Clarke, Coord. Chem. Rev. 232 (2002) 69–93.
[5] B. Rosenberg, L. Van Camp, T. Krigas, Nature 205 (1965) 698–699.
[6] B. Rosenberg, L. Van Camp, E.B. Grimley, A.J. Thomson, J. Biol. Chem. 246 (1967) 1347–1352.
[7] L. Kelland, Nat. Rev. 7 (2007) 573–584.
[8] B. Lippert, Coord. Chem. Rev. 182 (1999) 263–295.
[9] U. Kalinowska-Lis, J. Ochocki, K. Matlawska-Wasowska, Coord. Chem. Rev. 252 (2008) 1328–1345.
[10] G.N. Kaluđerović, S. Gómez -Ruiz, D. Maksimović-Ivanić, R. Paschke, S. Mijatović, Bioneorg. Chem. Appl. (2012), http://dx.doi.org/10.1155/2012/140284 article ID 140284, 14 pages.
[11] M.A. Jakupec, M. Galanski, B.K. Keppler, Rev. Physiol. Biochem.. Pharmacol. 146 (2003) 1–53.
[12] G.N. Kaluđerović, R. Paschke, Curr. Med. Chem. 48 (2011) 4738–4752.
[13] S. Gómez, D. Maksimović-Ivanić, S. Mijatović, G.N. Kaluđerović, Article ID 140284, Bioinorg. Chem. Appl. (2012) 1–14.
[14] I. Ott, Coord. Chem. Rew 253 (2009) 1670–1681.
[15] K.C. Dash, H. Schmidbauer, Metal Ions in Biological Systems, Marcel Dekker, New York, 1982.
[16] A. Casini, M.A. Cinellu, G. Minghetti, C. Gabbiani, M. Coronnello, E. Mini, L. Messori, J. Med. Chem. 49 (2006) 5524–5531.
[17] D. Aldinucci, D. Lorenzon, L. Stefani, L. Giovagnini, A. Colombatti, D. Fregona, Anti-Cancer Drug 18 (2007) 323–332.
[18] M. Coronnello, G. Marcon, S. Carotti, B. Caciagli, E. Mini, T. Mazzei, P. Orioli, L. Messori, Oncol. Res. 12 (2001) 361–371.
[19] L. Messori, F. Abbate, G. Marcon, P. Orioli, M. Fontani, E. Mini, T. Mazzei, S. Carotti, T. O'Conell, P. Zanello, J. Med. Chem. 43 (2000) 3541–3548.
[20] A. Bindoli, M.P. Rigobello, G. Scutari, C. Gabbiani, A. Casini, L. Messori, Coord. Chem. Rev. 253 (2009) 1692–1707.
[21] S. Nobili, E. Mini, I. Landini, C. Gabbiani, A. Casini, L. Messori, Med. Res. Rev. 105 (2010) 550–580.
[22] A. Casini, C. Hartinger, C. Gavviani, E. Mini, P.J. Dyson, B.K. Keppler, L. Messori, J. Inorg. Biochem. 102 (2008) 564–575.
[23] G. Marson, S. Carotti, M. Coronnello, L. Messori, E. Mini, P. Orioli, T. Mazzei, M.A. Cinellu, G. Minghetti, J. Med. Chem. 45 (2002) 1672–1677.
[24] F. Abbate, P. Orioli, B. Bruni, G. Marson, L. Messori, Inorg. Chim. Acta 311 (2000) 1–5.
[25] T. Yang, J.Y. Zhang, C. Tu, J. Lin, Q. Liu, Z.J. Guo, J. Inorg. Chem. 19 (2003) 45–48.
[26] B.Đ. Glišić, U. Rychlewska, M.I. Djuran, Dalton Trans. 41 (2012) 6887–6901.
[27] S.J. Berners-Price, A. Filipovska, Metallomics 3 (2011) 863–873.
[28] C.-M. Che, R.W.-Y. Sun, W.-Y. Yu, C.-B. Ko, N. Zhu, H. Sun, Chem. Commun. (2003) 1718–1719.
[29] S. Nobilli, E. Mini, I. Londini, C. Gabbiani, A. Casini, L. Messori, Med. Res. Rew 30 (2010) 550–580.
[30] R.V. Parish, B.P. Howe, J.P. Wright, J. Mack, R.G. Pritchard, R.G. Buckley, A.M. Elsome, S.P. Fricker, Inorg. Chem. 35 (1996) 1659–1666.
[31] R.G. Buckley, A.M. Elsome, S.P. Fricker, G.R. Henderson, B.R.C. Theobald, R.V. Parish, B.P. Howe, L.R. Kelland, J. Med. Chem. 39 (1996) 5208–5214.
[32] L. Ronconi, L. Giovagnini, C. Marzano, F. Bettio, R. Graziani, G. Pilloni, D. Fregona, Inorg. Chem. 44 (2005) 1867–1881.
[33] C.T. Lum, Z.F. Yang, H.Y. Li, R.W.-Y. Sun, S.T. Fan, R.T.P. Poon, M.C.M. Lin, C.-M. Che, H.F. Kung, Int. J. Cancer 118 (2006) 1527–1538.
[34] K.H.-M. Chow, R.W.-Y. Sun, J.B.B. Lam, C.K.-L. Li, A. Xu, D.-L. Ma, R. Abagyn, Y. Wang, C.-M. Che, Cancer Res. 70 (2010) 329–337.
[35] J.J. Yan, A.L.-F. Chow, C.-H. Leung, R.W.-Y. Sun, D.-L. Ma, C.-M. Che, Chem. Commun. 46 (2010) 3893–3895.
[36] R.W.-Y. Sun, C.-N. Lok, T.T.-H. Fong, C.K.-L. Li, Z.F. Yong, T. Zau, A.F.-M. Siu, C.-M. Che, Chem. Sci. 4 (2013) 1979–1988.
[37] N. Pantelić, B.B. Zmejkovski, J. Trifunović-Macedoljan, A. Savić, D. Stanković, A. Damjanović, Z. Juranić, G.N. Kaluđerović, T.J. Sabo, J. Inorg. Biochem. 128 (2013) 146–153.
[38] B.B. Krajčinović, G.N. Kaluđerović, D. Steinborn, H. Schmidt, Ch Wagner, Ž. Žižak, Z.D. Juranić, S.R. Trifunović, T.J. Sabo, J. Inorg. Biochem. 102 (2008) 892–900.

[39] K. Nakamoto, Infrared and Raman Spectra of Inorganic and Coordination Compounds, Willey Interscience, New York, 1986.
[40] B.B. Zmejkovski, G.N. Kaluđerović, S. Gómez -Ruiz, Ž. Žižak, D. Steinborn, H. Scmidt, R. Paschke, Z.D. Juranić, T.J. Sabo, Eur. J. Med. Chem. 44 (2009) 3452–3458.
[41] G.P. Vasić, V.V. Glodjović, I.D. Radojević, O.D. Stefanović, L.R. Čomić, V.M. Djinović, S.R. Trifunović, Inorg. Chim. Acta 363 (2010) 3606–3610.
[42] N. Pantelić, B.B. Zmejkovski, T.P. Stanojković, V.V. Jeftić, G.P. Radić, S.R. Trifunović, G.N. Kaluđerović, T.J. Sabo, J. Serb. Chem. Soc. 79 (2014) 649–658.
[43] A.A. Isab, M.N. Shaikh, M. Monium-ul-Mehboob, B.A. Al-Maythalony, M.I.M. Wazeer, S. Altuwaijri, Spectrochim. Acta A 79 (2011) 1196–1201.
[44] K. Esumi, M. Nawa, N. Aihara, K. Usui, New. J. Chem. 22 (1998) 719–720.
[45] G.N. Kaluđerović, H. Schmidt, S. Schwieger, Ch Wagner, R. Paschke, A. Dietrich, T. Müller, D. Steinborn, Inorg. Chim. Acta 361 (2008) 1395–1404.
[46] G.N. Kaluđerović, H. Schmidt, D. Steinborn, T.J. Sabo, in: J.G. Hughes, A.J. Robinson (Eds.), Inorganic Biochemistry: Research Progress, Nova Science Publishers, Inc. Hauppauge, New York, 2008, pp. 305–326.
[47] G.N. Kaluđerović, H. Kommera, S. Schwieger, H. Schmidt, A. Paethanom, M. Kunze, R. Paschke, D. Steinborn, Dalton Trans. (2009) 10720–10726.
[48] G.N. Kaluđerović, S.A. Mijatović, B.B. Zmejkovski, M.Z. Bulatović, S. Gómez-Ruiz, M.K. Mojić, D. Steinborn, DjM. Miljković, H. Schmidt, S.D. Stošić-Grujičić, T.J. Sabo, D.D. Maksimović-Ivanić, Metallomics 4 (2012) 979–987.
[49] B.Đ. Glišić, Z.D. Stanić, S. Rajković, V. Kojić, G. Bogdanović, M.I. Đuran, J. Serb. Chem. Soc. 78 (2013) 1911–1924.
[50] R. Gust, B. Schnurr, R. Krauser, G. Bernhardt, M. Koch, B. Schmid, E. Hummel, H. Schoenenberger, J. Cancer Res. Clin. 124 (1998) 585–597.
[51] A.N. Wein, A.T. Stockhausen, K.I. Hardcastle, M.R. Saadein, S. Peng, D. Wang, D.M. Shin, Z. Chen, J.F. Eichler, J. Inorg. Biochem. 105 (2011) 663–668.
[52] Z.D. Hudson, C.D. Sanghvi, M.A. Rhine, J.J. Ng, S.D. Bunge, K.I. Hardcastle, M.R. Saadein, C.E. MacBeth, J.F. Eichler, Dalton Trans. 28 (2009) 7473–7480.
[53] R.W.-Y. Sun, C.-M. Che, Coord. Chem. Rev. 253 (2009) 1682–1691.
[54] K. Palanichamy, A.C. Ontko, Inorg. Chim. Acta 359 (2006) 44–52.
[55] W. Bal, J. Christodoulou, P.J. Sadler, A. Tucker, J. Inorg. Biochem. 70 (1998) 33–39.
[56] G. Marcon, L. Messori, P. Orioli, M.A. Cinellu, G. Minghetti, Eur. J. Biochem. 270 (2003) 4655–4661.
[57] B.P. Espósito, R. Najjar, Coord. Chem. Rev. 232 (2002) 137–149.
[58] B.Đ. Glišić, M.I. Djuran, Z.D. Stanić, S. Rajković, Gold Bull. 47 (2014) 33–40.
[59] X. Shi, D. Li, J. Xie, S. Wang, Z. Wu, H. Chen, Chin. Sci. Bull. 57 (2012) 1109–1115.
[60] Z.F. Chen, Y.C. Liu, Y. Peng, X. Hong, H.H. Wang, M.M. Zhang, H. Liang, J. Biol. Inorg. Chem. 17 (2012) 247–261.
[61] G. Brauer, Handbook of Preparative Inorganic Chemistry, vol. 1, Academic Press, New York, 1963.
[62] M.J. Frisch, G.W. Trucks, H.B. Schlegel, G.E. Scuseria, M.A. Robb, J.R. Cheeseman, G. Scalmani, V. Barone, B. Mennucci, G.A. Petersson, H. Nakatsuji, M. Caricato, X. Li, H.P. Hratchian, A.F. Izmaylov, J. Bloino, G. Zheng, J.L. Sonnenberg, M. Hada, M. Ehara, K. Toyota, R. Fukuda, J. Hasegawa, M. Ishida, T. Nakajima, Y. Honda, O. Kitao, H. Nakai, T. Vreven, J.A. Montgomery Jr., J.E. Peralta, F. Ogliaro, M. Bearpark, J.J. Heyd, E. Brothers, K.N. Kudin, V.N. Staroverov, R. Kobayashi, J. Normand, K. Raghavachari, A. Rendell, J.C. Burant, S.S. Iyengar, J. Tomasi, M. Cossi, N. Rega, J.M. Millam, M. Klene, J.E. Knox, J.B. Cross, V. Bakken, C. Adamo, J. Jaramillo, R. Gomperts, R.E. Stratmann, O. Yazyev, A.J. Austin, R. Cammi, C. Pomelli, J.W. Ochterski, R.L. Martin, K. Morokuma, V.G. Zakrzewski, G.A. Voth, P. Salvador, J.J. Dannenberg, S. Dapprich, A.D. Daniels, Ö. Farkas, J.B. Foresman, J.V. Ortiz, J. Cioslowski, D.J. Fox, Gaussian 09, Revision D.01, Gaussian, Inc., Wallingford, CT, 2009.
[63] C. Adamo, V. Barone, Chem. Phys. Lett. 274 (1997) 242–250.
[64] T.H. Dunning Jr., P.J. Hay, Modern Theoretical Chemistry, third ed., vol. 3, Plenum, New York, 1976, pp. 1–28.
[65] D. Andrae, U. Häußermann, M. Dolg, H. Stoll, H. Preuß, Theor. Chem. Acc. 77 (1990) 123.
[66] T. Mosmann, J. Immunol. Methods 65 (1983) 55–63.
[67] M. Ohno, T. Abe, J. Immunol. Methods 145 (1991) 199–203.
[68] R.H. Clothier, Methods Mol. Biol. 43 (1995) 109–118.
[69] N.K. Banada, W.C. Satterfield, A. Dunalp, K.S. Steimer, R. Kurrle, T.H. Finkel, Apoptosis 1 (1996) 69–84.